



Research Article

ISSN : 0975-7384  
CODEN(USA) : JCPRC5

**Amidolysis of phenylalanine-p-nitroanilide using TSA imprinted macromatric polymer catalysts: Effect of porogen on catalytic efficiency**

Divya Mathew<sup>1</sup>, Benny Thomas<sup>1,2</sup> and K. S. Devaky<sup>1\*</sup>

<sup>1</sup>School of Chemical Sciences, Mahatma Gandhi University, Kottayam, Kerala, India

<sup>2</sup>Department of Chemistry, St. Berchmans College (affiliated to Mahatma Gandhi University, Kottayam)  
Changanacherry, Kerala, India

**ABSTRACT**

Chymotrypsin mimics were synthesized by molecular imprinting technique using the transition state analogue phenyl-1-benzyloxycarbonylaminobenzyl phosphonate as the template, methacryloyl-L-histidine, and methacrylic acid as the functional monomers and EGDMA as the crosslinking agent. The TSA imprinted polymers were prepared in different porogens. Amidolysis of phenylalanine-p-nitroanilide was carried out using these TSA imprinted macromatric polymer catalysts. The investigations revealed that the porogen used in the polymerization reaction has a significant influence on the catalytic activity of the enzyme mimics in the amidolytic reactions. Morphological features of the polymer catalysts synthesized using DMSO and chloroform as the medium of polymerization were different. The macroporous polymer prepared in DMSO exhibited higher imprinting efficiency, enantioselectivity, and substrate shape specificity in amidolytic reactions compared to the less porous polymer catalyst prepared in chloroform. Pseudo first order kinetics was observed for the catalytic amidolysis.

**Key words:** Transition state analogues, TSA imprinted macromatric polymer catalysts, porogenic effect, tetrahedral oxyanion intermediate and amidase activity.

**INTRODUCTION**

Molecular imprinting technique is featured by the assembly of a highly crosslinked polymer matrix around a template molecule, utilizing its interactions with functional monomers to design a three-dimensional recognition site, complementary in both shape and functionality to the template [1-6]. Removal of the template molecules leave molecular imprints in the polymer network and are responsible for the binding specificity and lot of applications [7-10]. These imprints carry a functional and stereochemical “memory” and act analogous to catalytically active binding sites of biological enzymes or antibodies. Molecularly imprinted polymer catalysts have received considerable attention due to their thermal and pH stability and increased shelf life where natural enzymes may lose activity. The proteolytic enzyme chymotrypsin continues to be a good model of MIP catalysts (11-14). There are a large number of reports on the synthesis of chymotrypsin mimics by molecular imprinting techniques and investigations on their catalytic activity in hydrolytic reactions. The imprinting efficiency, catalytic activity, enantioselectivity, and substrate specificity of an enzyme mimic polymer catalyst is determined by various parameters like  $k_{obs}$ ,  $k_{obs}/k_{uncat}$  and  $k_{cat}$  etc. An efficient enzyme mimic require the use proper arrangement of functional groups (a complex, three-dimensional, steric arrangement of the functional groups) as in the case of natural enzymes.

**EXPERIMENTAL SECTION**

Z/Boc/Nphth-L-Phenylalanine, L-Histidine, benzyl carbamate, triphenylphosphite, 4-methoxybenzaldehyde and benzoyl chloride was purchased from SRL, Mumbai. Dicyclohexylcarbodiimide (DCC) and ethylene glycol

dimethacrylate (EGDMA) were purchased from Sigma Aldrich, USA. All chemicals used, other than listed above were from local suppliers, which were purified prior to use by following the standard procedures.

IR spectra were recorded on a Perkin-Elmer 1600 FT-IR spectrophotometer. Kinetic studies were performed using Shimadzu UV 2450 spectrophotometer. JEOL JSM6390 SEM analyzer was used for SEM analysis.  $^1\text{H}$  NMR spectra were taken using Bruker Advance DPX-300MHz FT-NMR spectrometer in  $\text{CDCl}_3$ .

### Synthesis of TSA

#### (Phenyl-1-benzyloxycarbonylamino-4-methoxybenzyl phosphonate)

The transition state analogue, phenyl-1-benzyloxycarbonylamino-4-methoxybenzyl phosphonate was synthesized by refluxing triphenyl phosphite (13.2mL), benzyl carbamate (13.2mmol), 4-methoxybenzaldehyde (19.8mmol) and glacial acetic acid (2mL) for 4 h at  $100^\circ\text{C}$  in an oil bath. The diphenylphosphonate formed was hydrolyzed with NaOH (0.4N), acidified with conc. HCl, filtered and purified by column chromatography [15]. **FTIR**:-1301  $\text{cm}^{-1}$  (P=O stretching), 946  $\text{cm}^{-1}$  (P-OH stretching) and 1252  $\text{cm}^{-1}$  (P-O-Bzl stretching).

### Synthesis of N-methacryloyl-L-histidine

N-methacryloyl-L-histidine was synthesized by treating methacryloyl chloride (1.95 mL in 3 mL DCM), L-histidine monohydrochloride (3.1g) and NaOH (0.8g) following the reported procedure [16, 17]. **FTIR (methanol)**:- 1611  $\text{cm}^{-1}$  (methacryl double bond), 1652  $\text{cm}^{-1}$  (amide carbonyl) and 1705 $\text{cm}^{-1}$  (acid carbonyl).

### Synthesis of TSA imprinted and non-imprinted polymers

The highly crosslinked bifunctional TSA imprinted enzyme mimic was prepared by radical initiated bulk polymerization of TSA, the functional monomers- methacryloyl L-histidine and methacrylic acid- and the crosslinker EGDMA in 1:2:9 molar ratio in  $\text{DMSO}/\text{CHCl}_3$  at  $80^\circ\text{C}$  for 8hrs. The template was completely leached out by washing with a mixture of 95mL methanol and 5mL 35% HCl. The corresponding non-imprinted enzyme mimic was also prepared by the same procedure without TSA [15, 17, 20].

### Synthesis of the substrate Z-L/D-phenylalanine-p-nitroanilide (Z-L/D-Phe-PNA)

A solution of Z-L/D-phenylalanine (0.01mol) and p-nitroaniline (0.01mol) in 30 mL ethyl acetate was stirred with a magnetic stirrer and cooled in an ice-water bath. Dicyclohexylcarbodiimide (0.01mol) in 30 mL ethyl acetate was added drop wise, the reaction mixture was stirred for 30 minutes in the ice water bath and the stirring was continued for another 3h at room temperature. The N, N-Dicyclohexylurea formed was filtered off and the filtrate was evaporated in vacuum. The residue obtained was recrystallized from hot ethanol containing 1% acetic acid. The substrates, t-Boc/Npht-L-phenylalanyl-p-nitroanilides were also prepared following the same procedure [17, 18].

### Amidolysis of Z-L-Phenylalanine-p-nitroanilide (Z-L-Phe-PNA) using TSA imprinted and non-imprinted enzyme mimics

A suspension of chymotrypsin mimic (10mg) in 5mL Acetonitrile-Tris HCl buffer (1:9 by volume, pH 7.75, 5mL) was taken in a reagent bottle, equilibrated for half an hour and 100 molar excess of the substrate anilide, Z-L-Phenylalanyl-p-nitroanilide (Z-Phe-PNA) in acetonitrile (50 mL) was added. The reaction mixture was placed in a water bath shaker at  $45^\circ\text{C}$  and shaken well. Amidolysis of Z-Phe-PNA was followed by monitoring the absorbance of released p-nitroaniline spectrophotometrically at 347 nm [19]. Amidase activity of all the mimics was evaluated in a similar manner in the framework of Michaelis-Menten kinetics and the amidolysis was monitored. A blank reaction without any polymer was also carried out. From the absorbance value, the rate constant and percentage amidolysis was evaluated.

## RESULTS AND DISCUSSION

### Synthesis of transition state analogue

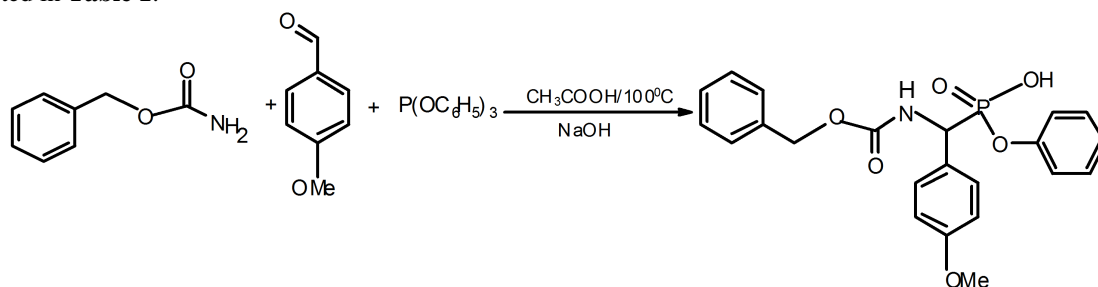
Rac-TSA was obtained by the acid catalyzed condensation of benzylcarbamate, 4-methoxybenzaldehyde and triphenyl phosphite [15]. The product was isolated and purified by column chromatography (**Scheme 1**).

**FTIR**: 1300  $\text{cm}^{-1}$  (P=O stretching), 945  $\text{cm}^{-1}$  (P-OH stretching), 1250  $\text{cm}^{-1}$  (P-O-benzyl stretching).  **$^1\text{H}$  NMR (400 MHz,  $\text{CDCl}_3$ ,  $\delta$ )**: 1.73(s, 2H,  $\text{CH}_2$ ), 3.77 (s, 3H,  $\text{OCH}_3$ ), 6.5-7.5(m, 14H, aromatic CH), 6.13(broad, 1H, NH), 6.09(m, 1H, CH).

### Synthesis of TSA imprinted and non-imprinted polymers (P1-P4)

The super cross-linked imprinted polymer with crystal-clear recognition sites was prepared by radical polymerization method in DMSO using N-methacryloyl-L-histidine and methacrylic acid as the functional monomers, TSA as template and EGDMA as the cross linker (**Scheme. 2**). To investigate the effect of the medium of

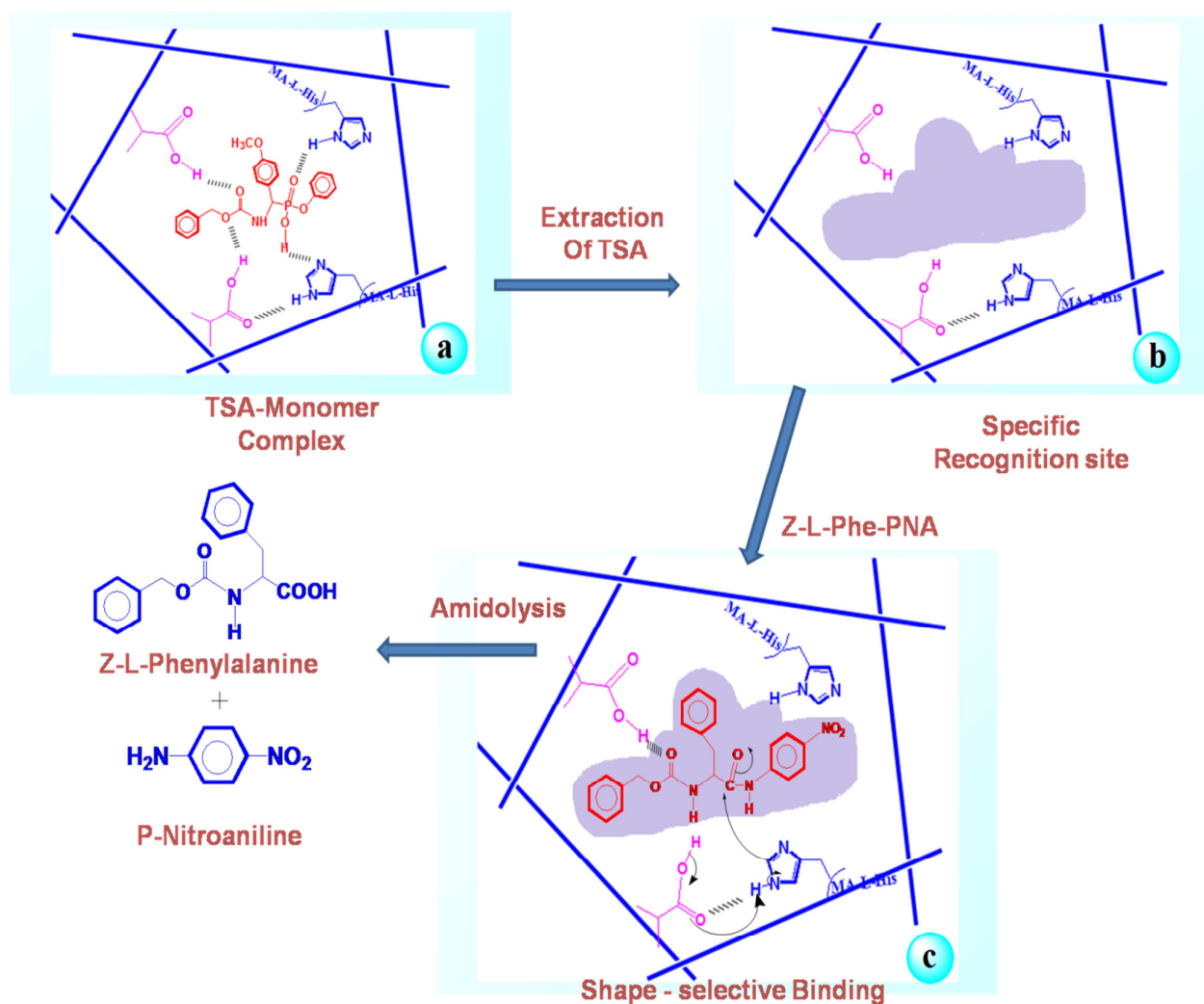
polymerization on imprinting and hence on amidolysis, imprinted and non-imprinted polymer catalysts were prepared in chloroform also. All polymers **P1–P4** were synthesized according to this general procedure. The details are listed in **Table 1**.



Scheme 1: Synthesis of transition state analogue

Table 1: Synthesis of Chymotrypsin mimics for the amidolysis of Z-L-Phe-PNA

Chymotrypsin mimics	TSA (gm)	Functional monomers		EGDMA (mL)	[Im] Mmol/g
		MA-L-His	MAA		
<b>P1</b> (DMSO)	0.407	0.2431	0.1156	14.804	0.894
<b>P2</b> (DMSO)	-	0.2431	0.1156	14.804	0.897
<b>P3</b> (CHCl <sub>3</sub> )	0.407	0.2431	0.1156	14.804	0.861
<b>P4</b> (CHCl <sub>3</sub> )	-	0.2431	0.1156	14.804	0.864



Scheme 2. Scheme for the synthesis and amidolysis of trifunctional enzyme mimic

The TSA molecules leave molecular imprints after being extracted from the polymer network. These molecular imprints act analogous to catalytically active binding sites of biological enzymes. The cavities in the molecularly imprinted polymer (MIP) are capable to recognize the substrate specifically and to stabilize the transition state of

the reaction, i.e., to lower the activation energy and thus, to accelerate the reaction. The imidazole content in the polymer matrix was estimated by cleaving the amino acid from the methacrylic backbone by refluxing with HCl and then treating with Ninhydrin reagent [17]. The 90% crosslinking makes the polymer network sufficiently rigid to maintain the recognition site and to accommodate the transition state of amidolysis by shape-selective binding. **FT-IR**:- 3456  $\text{cm}^{-1}$  (O–H stretching of carboxylic acid group), 3433  $\text{cm}^{-1}$  (NH stretching), 3142  $\text{cm}^{-1}$  (C–H stretching of imidazole ring), 1602  $\text{cm}^{-1}$  and 1445  $\text{cm}^{-1}$  (C=C and C=N stretching of imidazole ring).

The morphology of the polymers prepared in DMSO and  $\text{CHCl}_3$  was assessed by SEM analysis (**Fig. 1**). The surface of **P1** is full of cavities due to the removal of TSA molecules. The SEM picture of **P3** reveals that the porogen chloroform makes the imprinted polymer less porous.

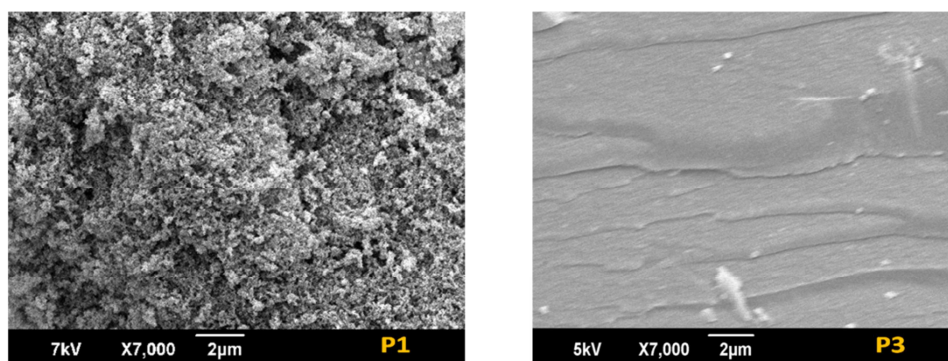


**Fig. 1.** SEM picture of the imprinted polymers prepared in DMSO and  $\text{CHCl}_3$

#### Catalytic activities of imprinted and non-imprinted polymers

The amidolysis of N-benzyloxycarbonyl phenylalanine-p-nitroanilide (Z-L-Phe-PNA) was carried out using **P1** (MIP) and **P2** (NIP) at 45 °C.

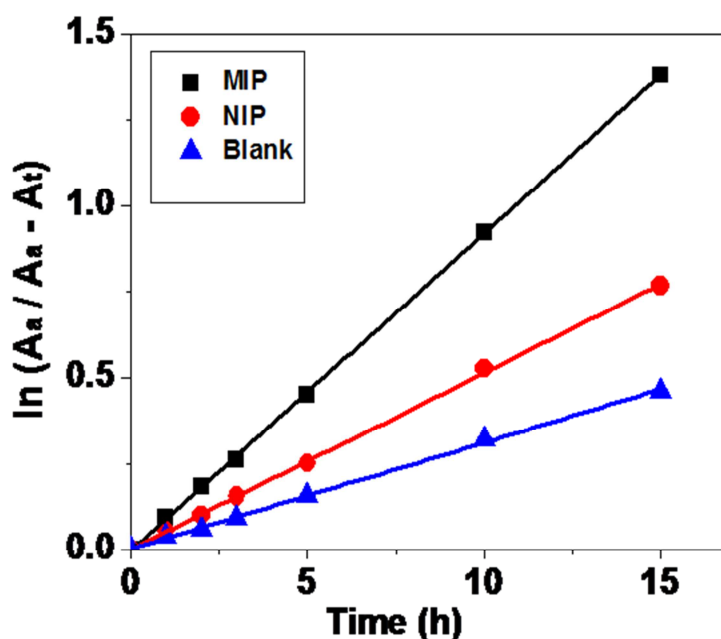


**Fig. 2.** Evaluation of rate constant for the amidolysis of anilide with TSA imprinted (MIP), non-imprinted (NIP) and uncatalyzed reaction

The imidazole moiety in the polymer matrix acts as the nucleophile for the amidolytic reaction. The carboxylic groups in the polymer matrix serve to stabilize the “tetrahedral oxyanion” transition state intermediate of the amidolytic reaction and further abstraction of a proton from the imidazole nitrogen enhances the nucleophilicity of the imidazole moiety (**Scheme 2c**). At lower pH the imidazole nitrogen gets protonated and its nucleophilicity gets lost. Hence, the pH of the reaction medium was maintained slightly alkaline (7.75) using Tris HCl buffer. The pseudo first order kinetics of the amidolytic reaction was evaluated using the equation  $k = \ln\{A_\infty/[A_\infty - A_t]\}$ , where  $A_\infty$  is the absorbance of the released p-nitroaniline at

infinite time and  $A_t$  is the absorbance at time  $t$ . Both **P1**, **P2** and uncatalyzed reaction follow pseudo first order kinetics (**Fig. 2**). Depending upon the nature of the porogen used for the polymerization, there is a remarkable difference in the rate of amidolysis of imprinted polymers. It is known that the nature of porogenic solvents determine the strength of non-covalent interactions and influences polymer morphology, which, obviously, directly affects the activity of enzyme mimics, especially that of MIPs. As described in the experimental section, the course of amidolytic reaction was monitored for **P1**, **P2**, **P3** and **P4** for the duration of 60 min and a plot of percent amidolysis vs. time is depicted in **Fig. 3**.

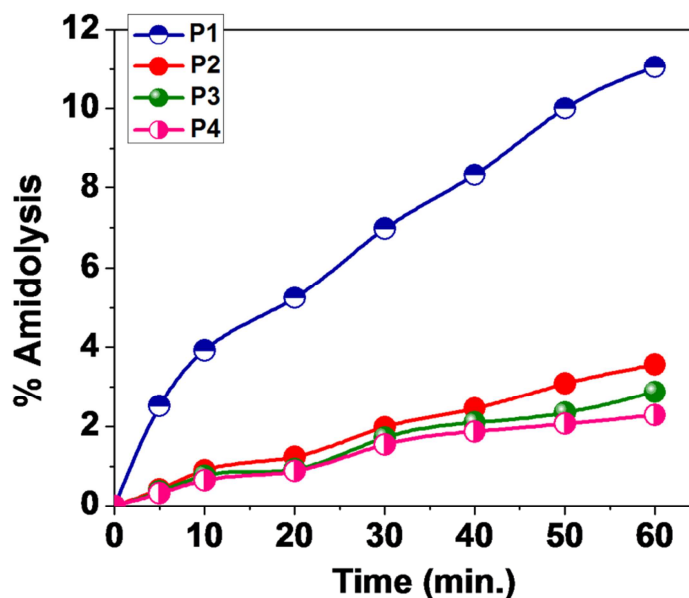


Fig. 3. Plot of percent amidolysis vs. time

Hundred-fold molar excess of Z-L-Phe-PNA over the amount of the key functional group- imidazole- was used. Among the polymer catalysts, **P1** shows initial burst kinetics, as enzyme catalysis under Michaelis- Menten framework, but takes much more time for attaining saturation, compared to natural chymotrypsin. Amidolysis of Z-L-Phe-PNA is catalyzed by the catalysts **P2**, **P3** and **P4** comprising of MA-histidine and methacrylic acid; it follows pseudo first-order kinetics without any burst. With polymer **P1**, approximately 55% of the amidolysis of Z-L-phenylalanine *p*-nitroanilide took place within 35h. But, less than 30% amidolysis took place with the polymer **P3** even after 7 days. The time taken for attaining saturation of the amidolysis reaction for **P3** is four times than that of **P1**, which indicates that the use of thermodynamically good solvent tends to lead to polymers with well-developed pore structures and use of a thermodynamically poor solvent leads to polymers with poorly developed pore structures.

The observed rate constant for the uncatalyzed reaction is only  $5.2 \times 10^{-4} \text{ min}^{-1}$ . The rate of amidolysis catalyzed by **P1** ( $2.11 \times 10^{-3} \text{ min}^{-1}$ ) is higher than that of **P2** ( $8.4 \times 10^{-4} \text{ min}^{-1}$ ) and it represents the imprinting effect. During imprinting, the TSA creates a tetrahedral geometry similar to the tetrahedral T.S of hydrolysis. The catalytic functions provide accommodation of the substrate anilide into the 3D cavity by stabilizing the T.S through effective H-bonding. In **P2**, the catalytic entities are not precisely fabricated due to the lack of TSA and exhibits relatively low rate of acceleration. The higher value of  $k_{obs.} / k_{uncat}$  exhibited by **P1** (4.06) compared to **P2** (1.62) is definitely due to the imprinting effect. Furthermore, the higher 1.20 times rate acceleration shown by **P3** ( $0.61 \times 10^{-3} \text{ min}^{-1}$ ) than that of **P4** ( $0.57 \times 10^{-3} \text{ min}^{-1}$ ) supports the imprinting effect on catalytic amidolysis (**Table 2**).

The imprinting efficiency of the enzyme mimics prepared was evaluated using the equation  $k_{cat} = [k_{obs} - k_{uncat}] / [Im]$ . The negligibly small value of imprinting competence  $k_{cat}$  exhibited by the **P3** ( $1.05 \times 10^{-2} \text{ mmol}^{-1} \text{ min}^{-1}$ ) is mainly due to the less porous nature of the polymer matrix. The higher value of imprinting efficiency shown by **P1** ( $17.79 \times 10^{-2} \text{ mmol}^{-1} \text{ min}^{-1}$ ) compared to **P3** ( $1.05 \times 10^{-2} \text{ mmol}^{-1} \text{ min}^{-1}$ ) and the higher  $k_{cat}$  value exhibited by **P2** ( $3.57 \times 10^{-2} \text{ mmol}^{-1} \text{ min}^{-1}$ ) and **P4** ( $0.58 \times 10^{-2} \text{ mmol}^{-1} \text{ min}^{-1}$ ) is most probably due to the formation of macroporous polymer matrix in **P1** and **P2**. During imprinting, the polar aprotic DMSO stabilizes the H-bonding between the TSA-monomer complexes. Moreover, the higher activity of the MIPs can be attributed to the presence of molecular imprints, which had been formed by the immobilized TSA-template molecules during polymerization.

**Table 2:** Kinetic parameters for the amidolysis Z-L-Phe-PNA using TSA imprinted and non-imprinted enzyme mimics in DMSO (P1 and P2) and CHCl<sub>3</sub> (P3 and P4)

Chymotrypsin mimics	$10^3 k_{obs.} \text{ min}^{-1}$	$k_{obs.} / k_{uncat.}$	$10^2 (k_{cat})^{\#}$	Saturation Time(hour)
<b>P1</b>	2.11	4.06	17.79	35
<b>P2</b>	0.84	1.62	3.57	120
<b>P3</b>	0.61	1.17	1.05	120
<b>P4</b>	0.57	1.10	0.58	120

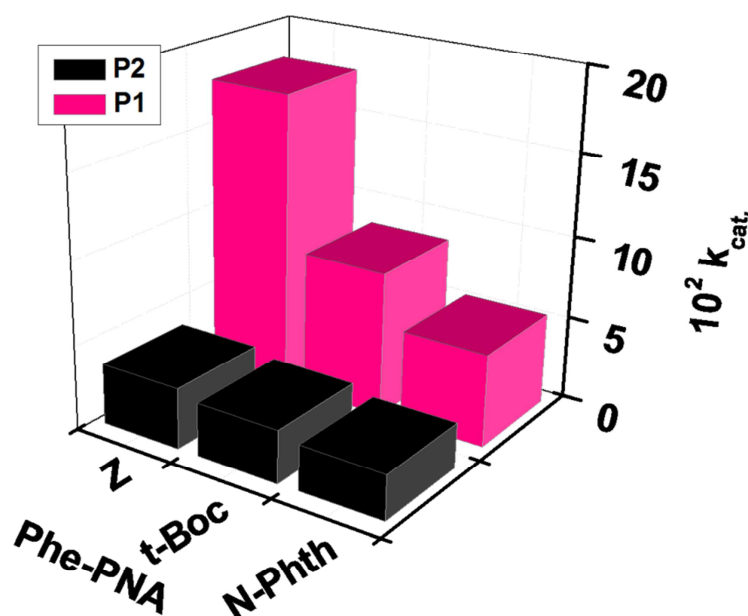
$$* \text{Catalytic efficiency, } \# \text{ imprinting efficiency of the enzyme mimic and } k_{cat} = \frac{[k_{MIP} - k_{uncat}]}{[Im]}$$

### Enantioselectivity of TSA imprinted polymers

The enantioselectivity studies of the enzyme mimics were carried out using Z-L-Phe-PNA and Z-D-Phe-PNA and the results were listed in **Table 3**, which clearly indicates that the TSA imprinted polymer exhibits efficient enantioselectivity than that of the non-imprinted polymers. The L- TSA from the rac-TSA selectively forms pre-polymerization complex with methacryloyl-L- histidine and methacrylic acid that is stabilized by H-bonding. Consequently, the imprinted cavity keeps the shape and configuration of L-TSA in memory and enantioselectivity binds L-enantiomer of Z-Phe-PNA predominantly over the D-enantiomer recognizing its L-configuration [19, 20]. The enantioselectivity ratio  $k_L/k_D$  for **P1**, made with DMSO as porogen is 4.51 and for **P3** made with chloroform as porogen is only 1.50. The polymer **P1** exhibits 3.00 fold greater enantioselectivity than that shown by **P3**. This explains the role of porogen in creating the macro porous structure in the polymer matrix and thus the resulting catalytic activity and enantioselectivity. The poor enantioselectivity shown by **P3** is due to its less porous polymer matrix and hence poor swelling in ACN-Tris HCl buffer.

**Table 3:** Kinetic parameters for the enantioselective amidolysis of Z-L/D-Phe-PNA using chymotrypsin mimics prepared in DMSO and CHCl<sub>3</sub>

Chymotrypsin mimics	$10^3 k_{obs.}^L$	$\frac{k_{obs.}^L}{k_{uncat.}^L}$	$10^2 k_{cat.}^L$	$10^3 k_{obs.}^D$	$\frac{k_{obs.}^D}{k_{uncat.}^D}$	$k_{cat.}^D$	$\frac{k_{cat.}^L}{k_{cat.}^D}$
<b>P1</b>	2.11	4.06	17.79	1.72	3.74	3.94	4.51
<b>P2</b>	0.84	1.62	3.57	0.64	1.39	2.01	1.78
<b>P3</b>	0.61	1.17	1.05	0.52	1.13	0.70	1.50
<b>P4</b>	0.62	1.19	1.16	0.54	1.17	0.93	1.25

**Fig. 4.** Comparison of catalytic activity of P1 and P2 in shape - selective amidolysis

### Substrate selectivity of TSA imprinted polymers

The imprinted polymer catalyst could recognise the structure of the TSA, especially the benzyloxycarbonyl group and the benzyl side chain of the anilide and selectively bind the structurally related p-nitroanilide. In order to investigate the substrate selectivity of TSA imprinted polymer catalytic amidolysis of structurally related p-nitroanilides-Z/t-Boc/ N-

Phth -L-Phe-PNA- was carried out. The polymer **P1** exhibited the highest catalytic efficiency ( $k_{MIP}/k_{unecat}$ ) of 4.06 towards Z-L-Phe-PNA, but it shows lower activity in the amidolysis of Boc-L-Phe-PNA ( $2.64 \times 10^{-3} \text{min}^{-1}$ ) and more sterically hindered N-Phth -L-Phe-PNA ( $2.23 \times 10^{-3} \text{min}^{-1}$ ). Hence, the imprinted polymer catalyst is capable of exhibiting efficient selectivity in its amidolytic catalysis because it recognizes the structure of imprinted molecule and selectively catalyse the substrate that has a similar structure as that of the imprinted TSA molecule. But, **P2** -the non-imprinted molecule, due to the lack of imprinted sites, show negligibly small catalytic efficiency compared to **P1** - 1.62, 1.60 and 1.59 respectively in the amidolysis of Z/t-Boc/ N-Phth -L-Phe-PNA(**Fig. 4**).

The porosity and as a consequence the swelling of the polymer matrix affects the imprinting efficiency- the role of size and shape of the “memorized cavity” in governing the selectivity of amidolysis.

**Table 4: Kinetic parameters for the shape – selective amidolysis of various N-protected L- Phe-PNA by chymotrypsin mimics prepared in DMSO and  $\text{CHCl}_3$**

Chymotrypsin mimics	Substrate	$10^3 k_{unecat} \text{min}^{-1}$	$10^3 k_{obs} \text{min}^{-1}$	$k_{obs}/k_{unecat}$	$10^2 k_{cat} \text{min}^{-1} \text{mmol}^{-1}$
<b>P3</b>	Z-L-Phe-PNP	0.52	0.61	1.17	1.05
	<i>t</i> -Boc-L-Phe-PNP	0.47	0.54	1.15	0.81
	N-Phth-L-Phe-PNP	0.40	0.44	1.10	0.46
<b>P1</b>	Z-L-Phe-PNP	0.52	2.11	4.06	17.79
	<i>t</i> -Boc-L-Phe-PNP	0.47	1.24	2.64	8.61
	N-Phth-L-Phe-PNP	0.40	0.89	2.23	5.48

The macroporous polymer **P1** exhibits higher imprinting efficiency due to the greater accessibility of the catalytic sites to the substrate - Z-L- Phe-PNA ( $17.79 \times 10^{-2} \text{min}^{-1} \text{mmol}^{-1}$ ), *t*Boc-L-Phe-PNA ( $8.61 \times 10^{-2} \text{min}^{-1} \text{mmol}^{-1}$ ) and N-Phth -L-Phe-PNA ( $5.48 \times 10^{-2} \text{min}^{-1} \text{mmol}^{-1}$ ) - compared to the less porous polymer **P3**, which exhibits much less imprinting efficiency as Z-L- Phe-PNA ( $1.05 \times 10^{-2} \text{min}^{-1} \text{mmol}^{-1}$ ), *t*Boc-L-Phe-PNA ( $0.81 \times 10^{-2} \text{min}^{-1} \text{mmol}^{-1}$ ) and N-Phth -L-Phe-PNA ( $0.46 \times 10^{-2} \text{min}^{-1} \text{mmol}^{-1}$ ). For both **P1** and **P3**, the best rate acceleration is observed between Z-L-Phe-PNA and N-Phth -L-Phe-PNA which are 3.25 and 2.28 respectively (**Table 4**).

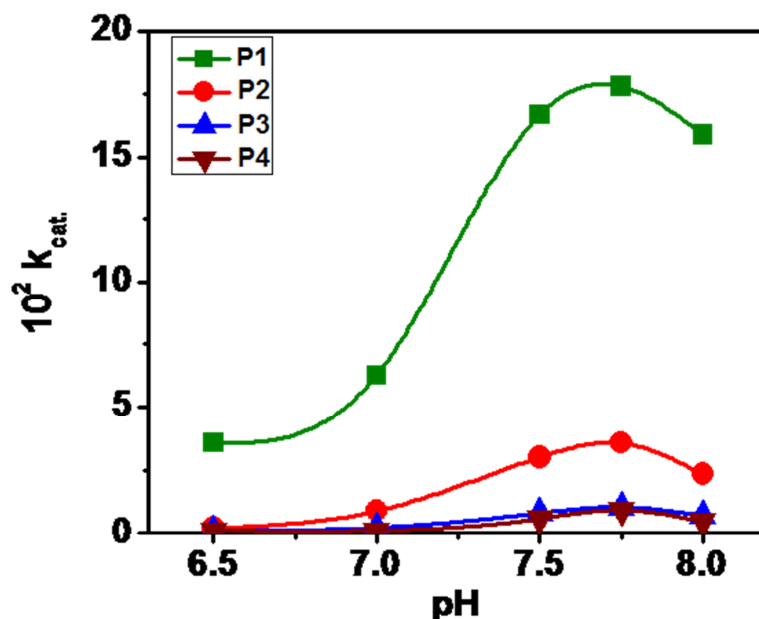


**Fig. 5.** The effect of pH on catalytic hydrolysis of chymotrypsin mimics

#### Effect of pH on the catalytic hydrolysis

The pH effect on the catalytic activity of the imprinted and non-imprinted copolymers prepared in DMSO (**P1** and **P2**) and chloroform (**P3** and **P4**) was studied in the pH range 6.5 - 8.0 in acetonitrile-Tris HCl buffer, and the results are depicted in **Fig. 5**. The catalytic activity of **P1** is very much higher than **P3**. Since the imidazole and carboxyl groups are brought into proximity in the polymer network through molecular imprinting it is well thought-out that significant enhancement in the amidolytic activity of **P1** in moderate pH is due to the cooperative effect induced by these catalytic functional groups. However, all the polymer catalysts follow the same pH profile that it exhibits an optimum rate at pH 7.75. The shrinkage or swelling of the polymer matrix took place on varying the pH of the reaction medium due to changes in number of protonated imidazole residues- the key catalytic

functionality- which resulted in decreased rate of amidolysis by the enzyme mimic. The catalytic activity of the polymer arises due to the neutral imidazole groups and as the pH of the reaction medium decreases protonation of imidazole nitrogen decreases the nucleophilicity. At lower pH even though the carboxylic acid groups are capable of forming efficient hydrogen bonds to the substrate, protonation of imidazole leads to decrease in the nucleophilicity of imidazole moieties. At higher pH all the polymers are abundant in negatively charged carboxylate ions, suggesting the possibility of the electrostatic exclusion of nucleophilic OH<sup>-</sup> from polymer-bound substrate and decrease in reaction rates were observed. At higher pH of the reaction medium, the rate of uncatalyzed reaction increased due to the increased concentration of hydroxyl ions.

#### Effect of solvent composition of reaction medium on catalytic amidolysis

The swelling of the polymer network is crucial for the easy access of the recognition sites and hence the composition of the solvent mixture plays a vital role on amidase activity of the imprinted polymer. In order to explore the outcome of the reaction medium on amidolysis, the reaction was carried out with different ratios of acetonitrile –Tris HCl buffer at pH 7.75 (Fig.6). The MIP **P1** shows significant decrease in imprinting efficiency ( $10^2 k_{cat}$ ) as the solvent composition (ACN-Tris HCl buffer) changes from 1:9 (17.79) to 3:7 (5.59) and then to 5:5 (0.1). Figure 6 implies that, as the acetonitrile content in the solvent mixture increases, the amidase activity of **P1** becomes similar to that of uncatalyzed reaction due to the swelling of the macroporous polymer **P1** in the medium. The molecular imprint with specific reactive functionalities gets deformed which limits the correct positioning of the T.S of the amidolysis in the cavity. At 5:5 ACN-Tris HCl buffer ratio, the catalytic efficiency ( $k_{obs}/k_{uncat}$ ) values shown by **P1** and **P2** were found to be 1.02 and 1.21 respectively implying that the imprinting effect is insignificant as the acetonitrile content in the reaction medium increases. In the case of **P3** and **P4**, catalytic efficiency increases as the ACN in the reaction medium increases. The recognition sites of the rigid polymer **P3** synthesized in chloroform were expected to be less deformed even though the ACN content in the solvent mixture increases. Moreover, the accessibility of the catalytic sites increases leading to remarkably higher imprinting efficiency ( $10^2 k_{cat}$ ) as the acetonitrile content in the solvent changes from 1:9 (1.05) to 5:5 (15.91).

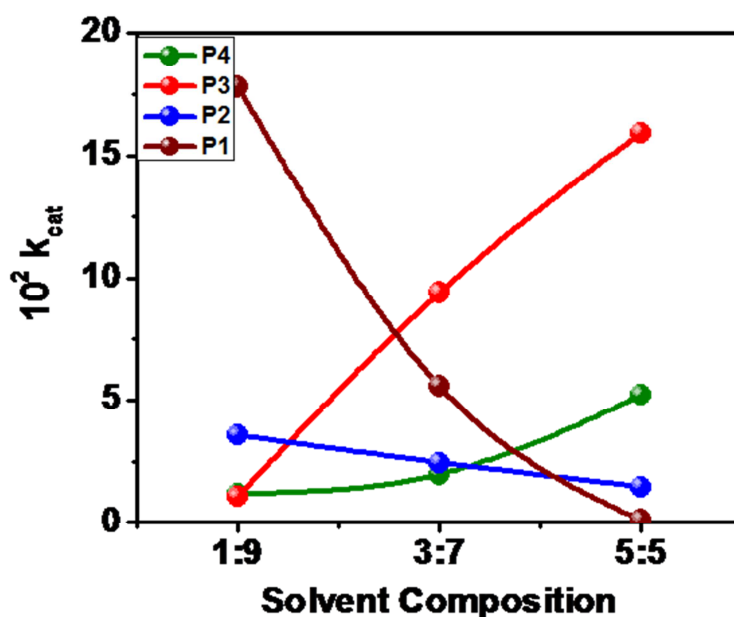


Fig. 6. Effect of solvent composition on catalytic amidolysis

The immobilization of the complementary functional groups in definite geometry during polymerization is responsible for the specificity of the imprinted polymer catalyst. The polymer **P3** prepared in chloroform as porogen resulted in less porous structure. When the percentage of acetonitrile is increased the imprinted polymer exhibited higher swelling capacity and then only the polymer can have well defined imprinted sites and hence increased catalytic activity. In 5:5 ACN- Tris HCl buffer, the efficiency of **P3** (15.91) is 160 times than that of **P1** (0.1). Thus, for **P1**, the best solvent composition is 1: 9 and for **P3**, it is found to be 9: 1. However, the amidase activity of **P1** in 1: 9 ACN- Tris HCl buffer is only 1.12 times higher than the amidase activity of **P3** in 9: 1 ACN- Tris HCl buffer. But the saturation time for **P1** in 1:9 ACN- Tris HCl buffer is only 35h while **P3** in 9:1 ACN- Tris HCl buffer did not show saturation in amidolysis even after 120h. Hence **P1** exhibits superior catalytic activity over **P3** (Fig. 7).

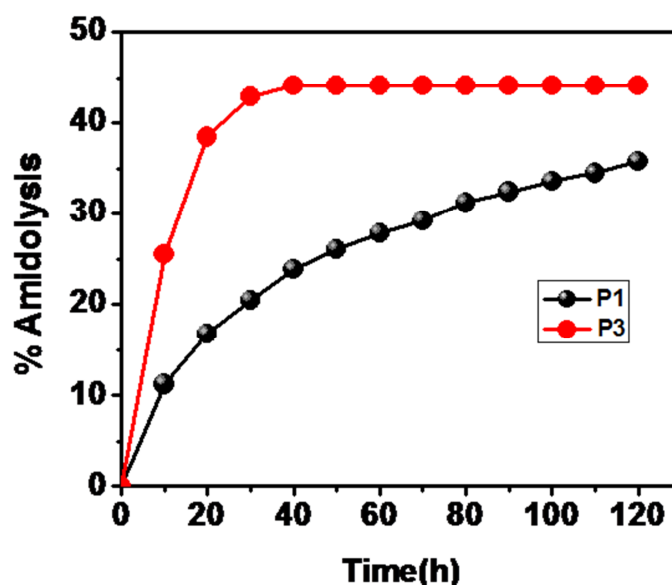


Fig. 7. Percentage amidolysis vs. time for P1 in 1:9 and P3 in 9:1 ACN- Tris HCl buffer

#### Effect of substrate concentration

The dependence of catalytic rate constant on substrate concentration was evaluated by carrying out the amidolysis reaction in different enzyme–substrate molar ratios (1:1, 1:50, 1:75, 1:100, 1:125, and 1:150). The rate of amidolysis was found to increase within the lower range of concentration of substrate and as the concentration of substrate is increased the rate decreased. The optimum molar ratio was found to be 1:100 and beyond this concentration catalytic activity decreased due to substrate inhibition which happens when two or more substrate molecules compete for the same active site at the same time (Fig. 8). When two substrate molecules are attached to the same catalytic centre, the enzyme becomes effectively inactive and gets subdued.

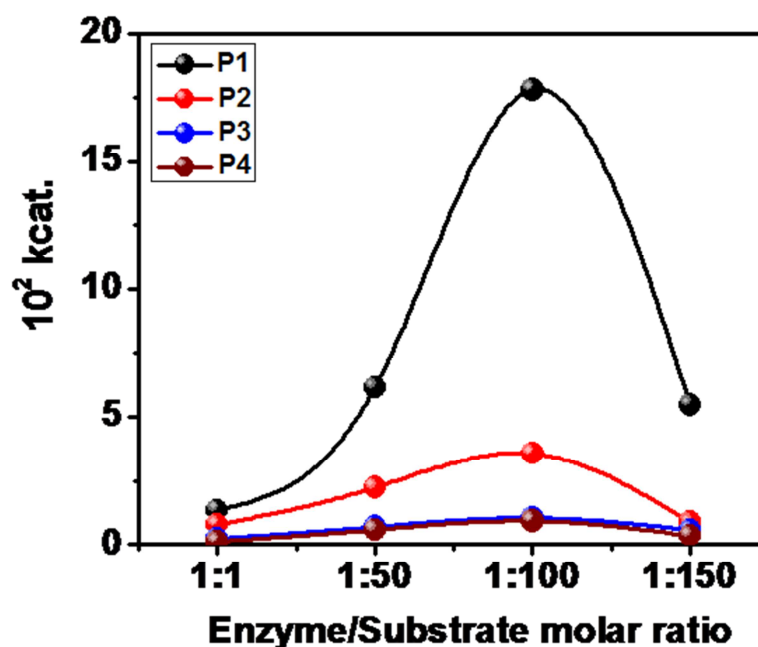


Fig. 8. The effect of substrate concentration on the amidolysis of Z-L-Phe-PNA by 90% EGDMA-crosslinked enzyme mimics prepared in DMSO and chloroform

As per Michaelis-Menten kinetics, the enzyme catalysis exhibits initial burst kinetics, substantial hasty increase in percentage amidolysis followed by saturation of its activity due to excess substrate. The amidase activity of the MIPs prepared in DMSO and chloroform was evaluated in the framework of Michaelis–Menten kinetics at pH 7.75. For this, the concentration of Z-L-Phe-PNA was taken in the range of 25–150-fold molar excess to that of the

polymer catalyst. The Michaelis-Menten plot shown in **Fig. 9** clearly indicates that, the initial rate was increased at first with increasing substrate concentration, but then leveled off at higher substrate concentration, and it remained constant when all recognition sites were occupied. The macroporous polymer network in **P1** provides great accessibility to bind the p-nitroanilide than the less porous polymer matrix in **P3** in 1:9 ACN- Tris HCl buffer. The catalyst **P3** could not behave like enzyme catalyzed reaction in 1: 9 ACN- Tris HCl buffer. But, in 9:1 ACN- Tris HCl buffer, a reverse trend is observed.

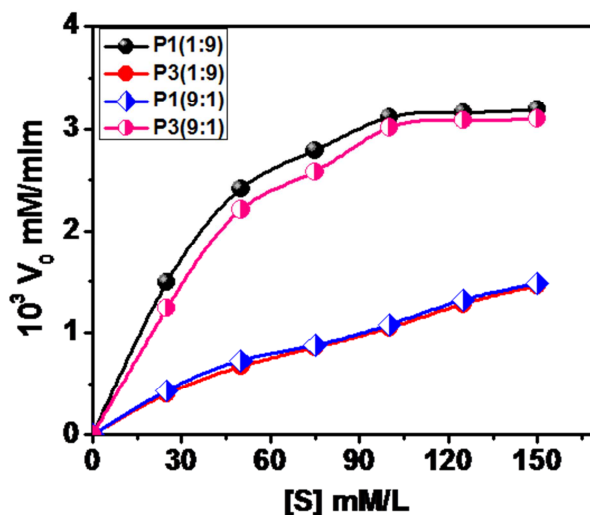


Fig. 9. Michaelis- Menten plot for the MIPs P1 and P3

#### Comparison with Natural Chymotrypsin

Compared to natural chymotrypsin, the polymer catalyst **P1** shows only 48% catalytic activity in the amidolysis of Z-L-Phe-PNA and it takes 35h for attaining saturation. But, it exhibits greater shelf life, higher thermal stability and can be recycled and reused on comparison with natural enzyme. The thermal stability of the enzyme mimics were investigated by incubating the imprinted mimics for 4 hours at a range of temperatures 90 °C-140 °C (**Table 5**).

Table 5: Kinetic parameters supporting thermal stability of MIPs

Chymotrypsin mimics	Kinetic parameters	Temperature °C						
		80	90	100	110	120	130	140
<b>P1</b>	$k_{obs}/k_{uncat}$	4.06	4.03	4.02	3.96	3.90	3.85	2.02
	$10^2 k_{cat}$	17.79	17.63	17.56	17.23	16.89	16.55	5.93
<b>P3</b>	$k_{obs}/k_{uncat}$	1.17	1.16	1.15	1.10	1.08	1.04	1.02
	$10^2 k_{cat}$	1.05	1.00	0.93	0.58	0.45	0.23	0.12

By measuring the catalytic parameters, it is found that, the enzyme mimics are stable up to 130 °C and then the catalytic activity gets decreased. A Sharp decrease in catalytic activity is observed for **P1** after 130 °C. But **P3** does not show considerable loss in catalytic activity up to 140 °C due to the rigid morphology of the polymer matrix. Natural chymotrypsin is denatured in the temperature range of 45 °C - 55 °C.

The reusability of the enzyme mimics in the amidolysis of Z-L-Phe-PNA was assessed in the framework of Michaelis-Menten kinetics at pH 7.75. **Table 6** shows the catalytic efficiency of both the MIPs for 5 consecutive amidolytic cycles. The results implies that after five cycles, the enzyme mimics exhibits **P1** (82%) and **P3** (55%) of its catalytic efficiency. The small decrease in catalytic activity observed after each cycle may be mainly due to the destruction of some the recognition sites. The better-quality reusability of the enzyme mimic presents a cost-based argument for its imminent role in economically feasible enzyme catalyzed process.

Table 6: Reusability of the spent MIP mimics

Chymotrypsin mimics	Kinetic parameters	No. of cycles of experiments				
		1	2	3	4	5
<b>P1</b>	$k_{obs}/k_{uncat}$	4.06	3.94	3.85	3.73	3.50
	$10^2 k_{cat}$	17.79	17.11	16.53	15.89	14.59
<b>P3</b>	$k_{obs}/k_{uncat}$	1.17	1.15	1.13	1.12	1.10
	$10^2 k_{cat}$	1.05	0.93	0.81	0.70	0.58

The amidolytic activity of the MIPs **P1** and **P3** were evaluated after one year of shelf life. The MIPs does not exhibit considerable loss in enzymatic activity in amidolysis even after one-year of shelf life (**Table 7**). The enzyme mimic **P1** shows only 3.82% decrease in imprinting efficiency while **P3** exhibits 11.43% decrease in imprinting efficiency.

**Table 7: Kinetic parameters supporting the higher shelf life of P1 and P3**

Chymotrypsin mimics	Kinetic parameters	Activity of fresh enzyme mimic	Activity after one year of shelf life
<b>P1</b>	$k_{\text{obs}}/k_{\text{uncat}}$	4.06	3.94
	$10^2 k_{\text{cat}}$	17.79	17.11
<b>P3</b>	$k_{\text{obs}}/k_{\text{uncat}}$	1.17	1.15
	$10^2 k_{\text{cat}}$	1.05	0.93

## CONCLUSION

Porogenic solvents have an eminent role in making the polymer matrix macroporous to assure good flow-through properties. The nature of porogens determines the strength of non-covalent interactions and the morphology of the imprinted polymer. The catalytic amidolysis shows that, for preparing an effective enzyme mimic with macroporous matrix DMSO is the best porogen, which leads to saturation within 35 hours. The polar, non-protic solvents stabilize the template-functional monomer complex by maximizing the H-bonding between the template and functional monomers. The polymer prepared in different porogens exhibits remarkable dependence on solvent composition ACN – Tris HCl buffer. The enzyme mimic prepared in CHCl<sub>3</sub> shows its maximum catalytic efficiency in 9:1 ACN – Tris HCl buffer while that prepared in DMSO shows the highest rate acceleration in 1:9 ACN – Tris HCl buffer.

## Acknowledgements

The authors gratefully acknowledge the support from CSIR for JRF and SRF (Divya Mathew). We are also thankful to IIRBS-Mahatma Gandhi University for providing facilities for spectral analysis and School of Biosciences for providing facilities for incubation studies.

## REFERENCES

- [1] K Mosbach. *Anal. Chim. Acta.*, **2001**, 435, 3-8.
- [2] K Mosbach; K Haupt. *J. Mol. Recogn.*, **1998**, 11, 62-68.
- [3] L Ye; K Mosbach. *React. Funct. Polymers*, **2001**, 48,149-157.
- [4] G Wulff. *Microchim Acta.*, **2013**, 180, 1149-1156.
- [5] K Flavin; M Resmini. *Anal. Bioanal. Chem.*, **2009**, 393, 437-444.
- [6] DJ Marty; Mauzac. *Adv. Polym. Sci.*, **2005**, 172, 1-35.
- [7] A Leonhardt; K Mosbach. *React. Polym.*, **1987**, 6, 285.
- [8] SA Zaidi. *Electrophoresis*, **2013**, 34, 1375-1381.
- [9] R Sancho; C Minguillón. *Chem. Soc. Rev.*, **2009**, 38, 797-806.
- [10] M Subat; AS Borovik; BJ König. *J. Am. Chem. Soc.*, **2004**,126, 3185-3192.
- [11] RL Schowen; JF Liebman; A Greenberg (Eds.), *Mechanistic Principles of Enzyme Activity*, VCH, New York, **1988**.
- [12] ML Bender; FJ Ke'zdy. *J. Am. Chem. Soc.*, **1964**, 86, 3704-3711.
- [13] T Kunitake; Y Okahata. *Adv. Polym. Sci.*, **1976**, 20, 159-168.
- [14] ML Bender; GR Schonbaum; GA Hamilton. *J. Polym. Sci.*, **1961**, 49, 75-83.
- [15] K Ohkubo; Y Urata; S Hirota; Y Funakoshi; T Sagawa; S Usui; K Yoshinaga. *J. Mol. Catal.*, **1995**, 101, L111-L114.
- [16] Y Okuda; M Yoshihara; T Maeshima. *Makromol. Chem. Rapid Commun.*, **1987**, 8, 579-586.
- [17] BS Lele; MG Kulkarni; RA Mashelkar. *React. Funct. Polym.*, **1999**, 40, 215-229.
- [18] J Jayaraman. *Laboratory Manual in Biochemistry*, Wiley Eastern, New Delhi, **1985**.
- [19] K Ohkubo; Y Funakoshi; T Sagawa. *Polymer*. **1996**, 37, 3993-3998.
- [20] K Ohkubo; K Sawakuma; T Sagawa. *J. Mol. Catal.*, **2001**, 165, 1-7.